# Optical absorption in random media: Application to $Ga_{1-x}Mn_xAs$ epilayers

J. Szczytko,[1] W. Bardyszewski,[2] and A. Twardowski[1]
[1]*Institute of Experimental Physics, Warsaw University, Hoża 69, 00-681 Warsaw, Poland*
[2]*Institute of Theoretical Physics, Warsaw University, Hoża 69, 00-681 Warsaw, Poland*
(Received 30 January 2001; published 17 July 2001)

A model to calculate the fundamental absorption edge in heavily doped semiconductors is proposed. The model is based on the assumption that the quasimomentum conservation rule in optical transitions is partially released in random media. This model is applied to transmission data of $Ga_{1-x}Mn_xAs$ epilayers. The values obtained for the free hole concentration $p=7\times10^{19}$ cm$^{-3}$, and the $p$-$d$ exchange integral $N_0\beta=-1$ eV reproduce reasonably well the fundamental absorption edge of $Ga_{1-x}Mn_xAs$.

DOI: 10.1103/PhysRevB.64.075306 PACS number(s): 78.40.Pg, 71.23.−k, 75.50.Pp

## I. INTRODUCTION

Understanding optical absorption in random media with broken translational symmetry is an important problem in semiconductor physics, to mention only heavily doped semiconductors and semiconductor based laser devices. It has been suggested that in order to describe the interband absorption in such systems the $\boldsymbol{k}$-conservation rule has to be relaxed, leading to so-called indirect transitions.[1–3]

Theoretical models of disorder in semiconductors are mainly concerned with the density of states in band tails due to the localization of electronic wave functions below the mobility edge.[4–6] Particularly fruitful in this respect was the concept of the optimal wave function of Halperin and Lax[7] which successfully explained the shape of the density of states in heavily doped semiconductors. Recently it has also been applied to the case of hydrogenated amorphous silicon,[8] giving very good agreement with experimental data. Effects of disorder in amorphous silicon were also studied using a microscopic model based on the tight binding approximation.[9] The probability of optical transitions between localized states is governed mainly by the densities of states in the valence and conduction bands, allowing for direct comparison of theoretical models with experimental results. The situation above the mobilty edge is quite different. In addition to the perturbation of the single-particle spectrum introduced by the disorder, we also have to take into account correlation phenomena of the optically generated electron-hole pairs. Even if we neglect the excitonic effects associated with electron-hole Coulomb interaction, which is a well justified assumption at high temperatures and concentrations of carriers, we still have to consider the correlation induced by the presence of the potential fluctuations. This is due to the fact that the optical generation of an electron-hole pair at a given point of the semiconductor depends on the particular form of the local potential. Consequently the spatially averaged absorption coefficient which is given by the two-particle propagator does not reduce to a convolution of single-particle densities of states. Therefore a model is needed that will at least approximately account for these effect in disordered media.

Recently a particular group of highly disordered systems has been attracting worldwide attention. These are mixed crystals based on III-V compounds such as GaAs, InAs, and GaSb, in which a controlled fraction of nonmagnetic cations is replaced by magnetic ions (the so-called diluted magnetic semiconductors, DMS's).[10] These materials are thought to be good candidates for spintronic devices due to their strong $s$, $p$-$d$ exchange interaction affecting their band structure and predicted ambient temperature ferromagnetism.[11,12]

The most reliable way to study the energy structure of III-V DMS's is magnetospectroscopy, covering the energy range from far infrared to near ultraviolet. Spectroscopy data in the range of the fundamental absorption edge, providing information about $s$, $p$-$d$ exchange, are so far nearly exclusively limited to $Ga_{1-x}Mn_xAs$. Several magnetic circular dichroism (MCD) experiments,[13,14] as well as direct absorption measurements,[15] were performed at the $\Gamma$ and $L$ points of the Brillouin zone. The absorption revealed a rather broad and structureless ramplike edge, while the MCD was found to be very sample dependent. Obviously standard direct optical transitions are not suitable to describe the experimental data.

In this paper we propose an approach to describing the fundamental absorption edge in disordered semiconductors, that is based on disorder induced partial relaxation of the $\boldsymbol{k}$-selection rule in direct transitions. This model includes both direct and indirect transition limits in a natural way. We show that the proposed approach can be used for description of highly $p$-type $Ga_{1-x}Mn_xAs$ magnetoabsorption data. In effect, the exchange parameter for the valence band can be estimated.

## II. THEORETICAL BACKGROUND

There are two standard approaches to calculating the absorption (or emission) due to band-to-band transition, which we briefly recall below.

The electron wave function in a perfect (periodic) crystal lattice is described by a Bloch wave function

$$\Psi_{\boldsymbol{k},\alpha}(\boldsymbol{r})=u_{\boldsymbol{k},\alpha}(\boldsymbol{r})e^{i\boldsymbol{k}\cdot\boldsymbol{r}}, \tag{1}$$

where $\boldsymbol{k}$ is the wave vector of the quasimomentum of the electron from the band $\alpha$. The standard formula for the absorption coefficient in three dimensional crystals (with excitonic effects neglected) can be written as[16]

 

$$\alpha(\omega)=\int \frac{d\boldsymbol{k}_c}{(2\pi)^3}\frac{d\boldsymbol{k}_v}{(2\pi)^3} M^2_{c,v}(\boldsymbol{k}_c,\boldsymbol{k}_v)\,\delta(\hbar\omega-E_g+E_v(\boldsymbol{k}_v) - E_c(\boldsymbol{k}_c))[f_v(E_v(\boldsymbol{k}_v))-f_c(E_c(\boldsymbol{k}_c))], \tag{2}$$

where $E_c(\boldsymbol{k}_c)$ and $E_v(\boldsymbol{k}_v)$ are the dispersion relations for the conduction and valence bands, $E_g$ is the energy gap, the Dirac $\delta$ denotes the conservation of the energy $\hbar\omega=E_g-E_v(\boldsymbol{k}_v)+E_c(\boldsymbol{k}_c)$, $f_v(E_v(\boldsymbol{k}_v))-f_c(E_c(\boldsymbol{k}_c))$ is the difference of the probabilities that the initial and final states involved in the transition are occupied (empty), and $M_{c,v}$ is the band-to-band transition matrix element.

For electrons described by the wave function given by Eq. (1) the matrix element $M_{c,v}$ is given by[1]

$$M^2_{c,v}(\boldsymbol{k}_c,\boldsymbol{k}_v)=A^2(2\pi)^3\delta(\boldsymbol{k}_c-\boldsymbol{k}_v). \tag{3a}$$

The coefficient $A$ for a zinc-blende type compound is given by

$$A^2=\frac{2\pi e^2\hbar E_p}{6cm_0\varepsilon_0\sqrt{\varepsilon_1}E}, \tag{3b}$$

where $E=\hbar\omega$, $E_p=2m_0P^2/\hbar^2$ with the interband matrix element $P$ introduced by Kane,[17] $\sqrt{\varepsilon_1}$ is the refractive index, $m_0$ is the free electron mass, $c$ is the velocity of light, and $e$ is the electron charge. Equation (3) describes standard direct transitions for which quasimomentum is conserved ($\boldsymbol{k}_c=\boldsymbol{k}_v$).

The situation is more complicated for heavily doped materials. According to the commonly accepted model,[1] the random distribution of impurities in a semiconductor host lattice breaks the translational symmetry of the crystal, so that the quasimomentum is not conserved in such a system. However, despite the full relaxation of the momentum conservation, the densities of states of the conduction and valence bands in this approach are taken like those in a perfect crystal. This means that the internal disorder totally relaxes the $\boldsymbol{k}$-vector selection rule, but only slightly modifies the energy band structure of the semiconductor. Due to the localized nature of the electronic states, they are delocalized in $\boldsymbol{k}$ space, so transitions between such states do not conserve quasimomentum. In the extreme case of the approach of Ref. 1 the matrix element $M^2_{c,v}$ is $\boldsymbol{k}$ independent,

$$M^2_{c,v}(\boldsymbol{k}_c,\boldsymbol{k}_v)=\text{const}=:B^2. \tag{4a}$$

The constant $B$ in the conventional theory can be derived from the so-called hydrogenic model, which assumes the presence of ionized impurities in the crystal, originating from shallow donors or acceptors:[1,2]

$$B^2=A^2 16\pi a^{*3}(1+a^{*2}k_b^2)^{-4}, \tag{4b}$$

where $a^*$ is the effective Bohr radius in the semiconductor and $k_b$ is an additional parameter (a sort of cutoff parameter) in the approach introduced by Eagles.[2]

In spite of the simplicity of that model, Eq. (4) was very successful in reproducing the gain spectra of semiconductor lasers.[1] Unfortunately this formula can be used in principle only for the localized states below the mobility edge. It turns out, however, that the hydrogenic formula can also be used for unintentionally doped semiconductors,[18,3] where the meaning of the parameter $k_b$ should be revised.

In general the $\boldsymbol{k}$-independent matrix element is used in heavily doped or heavily excited systems while in the case of semiconductor alloys the virtual crystal approximation (VCA) is often employed as a starting point. In the VCA approach the effective potential is taken as periodic and the $\boldsymbol{k}$ vector is still a good quantum number. The resulting band structure resembles that of the regular semiconductor. This suggests using quasimomentum conservation for the optical transitions [Eq. ( 3)], even though the translational symmetry is broken.

If one aims to calculate the band-to-band optical absorption, it is necessary to find a way to include the influence of the random potential fluctuations. We propose an approach that is more universal than that of Refs. 1 and 2 and extends beyond the VCA model. We consider the effect of long range fluctuations of the impurity concentration in heavily doped semiconductors on the optical absorption. It is assumed that the range of the perturbing potential introduced by a single defect or impurity is very small compared to the typical wavelength of band electron wave functions and that the wave functions change very little on a length scale equal to the typical distance between scattering centers. Consequently we can use the effective mass approximation.

For a disordered crystal the electron wave function cannot be described by a single Bloch plane wave [Eq. (1)]. We assume that for a real disordered crystal the electron wave functions can be described by a linear combination of the Bloch functions with different $\boldsymbol{k}$ vectors, forming in this way a packet with a certain wave vector distribution. Thus an electronic state can be characterized by the mean $\boldsymbol{k}$ vector $\boldsymbol{k}_0$ and the distribution of $\boldsymbol{k}$ vectors $\{\boldsymbol{k}\}$ around $\boldsymbol{k}_0$. With this meaning the dispersion relation $E(\boldsymbol{k}_0)$ of the mean $\boldsymbol{k}$ vector can still be defined in the crystal.

For optical transitions at least two electronic states with different energies are combined. Since both states are characterized by their $\boldsymbol{k}$ vector distributions, the effective squared matrix element $M^2_{c,v}$ is obtained by averaging with respect to those distributions. This procedure results in replacing the Dirac delta $\delta(\boldsymbol{k}_c-\boldsymbol{k}_v)$ in Eq. (3) by the distribution function of $\boldsymbol{k}$ vectors $\mathcal{D}(\boldsymbol{k}_c-\boldsymbol{k}_v)$. Thus

$$M^2_{c,v}(\boldsymbol{k}_c,\boldsymbol{k}_v)=A^2(2\pi)^3\mathcal{D}(\boldsymbol{k}_c-\boldsymbol{k}_v). \tag{5}$$

An analytical, exact expression for $\mathcal{D}(\boldsymbol{k}_c-\boldsymbol{k}_v)$ can be derived only from a microscopic model of the system. However, one might expect that for increasing density of the impurities in the crystal lattice (increasing disorder) $\mathcal{D}(\boldsymbol{k}_c-\boldsymbol{k}_v)$ should vary from the $\delta$-like distribution given by Eq. (3) to a distribution with increasing width. In the extreme case the distribution width becomes infinite and the matrix element $M_{c,v}$ becomes $\boldsymbol{k}$ independent [Eq. (4)]. In other words $\mathcal{D}(\boldsymbol{k}_c-\boldsymbol{k}_v)$ may be characterized by a width parameter $\sigma_k$ varying from 0 [Eq. (3)] to $\infty$ [Eq. (4)]. We propose to approximate the $\mathcal{D}(\boldsymbol{k}_c-\boldsymbol{k}_v)$ distribution by the following Gaussian function with $\boldsymbol{k}=[k_x,k_y,k_z]$:

$$\mathcal{D}(\boldsymbol{k}_c-\boldsymbol{k}_v)=\frac{1}{\sqrt{2\pi}\sigma_{kx}}\frac{1}{\sqrt{2\pi}\sigma_{ky}}\frac{1}{\sqrt{2\pi}\sigma_{kz}}\exp\left(-\frac{(k_{cx}-k_{vx})^2}{2\sigma_{kx}^2}-\frac{(k_{cy}-k_{vy})^2}{2\sigma_{ky}^2}-\frac{(k_{cz}-k_{vz})^2}{2\sigma_{kz}^2}\right). \quad (6)$$

Although our choice is arbitrary, it recovers the expected behavior of $\mathcal{D}(\boldsymbol{k}_c-\boldsymbol{k}_v)$ for large and small $\sigma_k$ and enables analytical calculation of the absorption coefficient as we will show below.

For simplicity we assume the isotropic energy versus wave vector relation $E(\boldsymbol{k})=E(|\boldsymbol{k}|)$, and isotropic broadening $\sigma_{kx}=\sigma_{ky}=\sigma_{kz}\equiv\sigma_k$. Then Eq. (5) reduces to

$$M_{c,v}^2(\boldsymbol{k}_c,\boldsymbol{k}_v)=A^2\left(\frac{2\pi}{\sigma_k^2}\right)^{3/2}\exp\left[-\frac{(\boldsymbol{k}_c-\boldsymbol{k}_v)^2}{2\sigma_k^2}\right]. \quad (7)$$

The broadening parameter $\sigma_k$ can be compared to the inverse of the characteristic localization length around imperfection present in the system. Comparing our approach to the hydrogenic model[1,2] at $\boldsymbol{k}_c=\boldsymbol{k}_v$ one finds

$$\sigma_k^3=\sqrt{\frac{\pi}{32}}\frac{(1+a^{*2}k_b^2)^4}{a^{*3}}. \quad (8a)$$

The average value of $(1+a^{*2}k_b^2)^{-4}$ for GaAs was found to be 0.87 at 77 K and 0.63 at 300K;[19] thus for GaAs

$$\sigma_k=\frac{0.7}{a^*}\approx\frac{1}{a^*}. \quad (8b)$$

In the hydrogenic model the $\sigma_k$ parameter corresponds to the inverse effective Bohr radius. This analogy may suggest the order of magnitude of $\sigma_k$. In a more general situation the parameter $\sigma_k$ may probably still be given by Eq. (8b) with $a^*$ understood as the characteristic localization length.

Assuming a parabolic dispersion relation expressed in terms of the average $\boldsymbol{k}_0$ vectors $E(k_0)=\hbar^2k_0^2/2m^*$ and for temperature sufficiently low so that $f_v-f_c\approx1$, one can simplify Eq. (7) as follows:

$$\alpha(\omega)=A^2\frac{2m_v}{(2\pi)^{5/2}\hbar^2\sigma_k}\int_0^{k_c^{max}}dk_c k_c\left[\exp\left(-\frac{1}{2\sigma_k^2}(k_c-k_v)^2\right)-\exp\left(-\frac{1}{2\sigma_k^2}(k_c+k_v)^2\right)\right], \quad (9a)$$

where

$$k_v=\sqrt{\frac{2m_v}{\hbar^2}\left(\hbar\omega-E_g-\frac{\hbar^2k_c^2}{2m_c}\right)} \quad (9b)$$

and

$$k_c^{max}=\sqrt{\frac{2m_v}{\hbar^2}(\hbar\omega-E_g-F)}, \quad (9c)$$

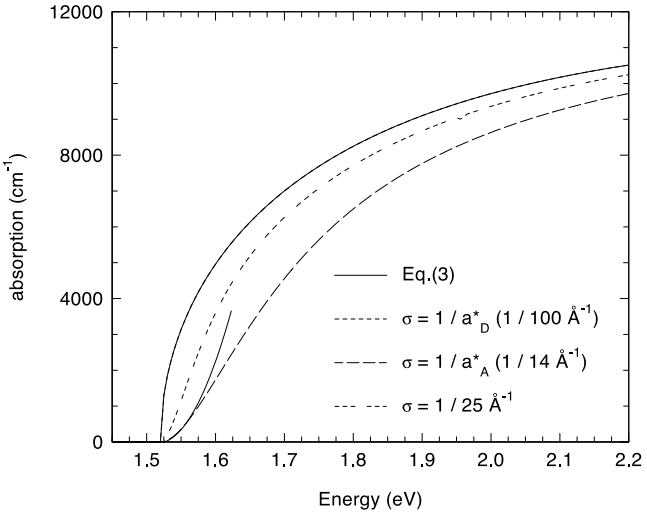


FIG. 1. The comparison between the fundamental absorption edge obtained from Eq. (3) (solid line) with the results derived from Eq. (9) for electron transition from heavy holes to the conduction band in GaAs. Isotropic and parabolic bands are assumed and excitonic effects are neglected. $\sigma_k$ parameters corresponding to the Bohr radius of the donor ($a_D^*=104$ Å) and of the acceptor ($a_A^*=14.8$ Å), and one for an object with size $a^*=25$ Å ($\sigma_k=4\times10^8$ m$^{-1}$) were used. For large values of $\sigma_k$ the beginning of the fundamental absorption edge is parabolic, which is consistent with the results of the model Eq. (4). Part of a parabola is also shown.

$m_c$ and $m_v$ are the masses of the electron in the conduction and valence bands, and $F$ is the Fermi energy in the presence of free holes measured relative to the top of the valence band ($F\geqslant0$).

The resulting absorption curves, in the absence of free carriers ($F=0$), are presented in Fig. 1. The fundamental absorption edge obtained from Eq. (3) within the direct transition approximation is compared to the results derived from Eq. (9) for electronic transition from heavy holes in the valence band to the conduction band in GaAs. For a value of $\sigma_k$ that corresponds to the Bohr radius of the donor [$a^*=104$ Å, Eq. (8)] there is almost no difference between the results of Eq. (3) and Eq. (9). However, when $\sigma_k$ increases and can be related to the size of the Bohr radius of the acceptor state ($a^*=14.8$ Å) the absorption spectrum is quite different. We note that for large $\sigma_k$ (no $\boldsymbol{k}$-selection rule) and photon energies close to the energy gap the absorption coefficient is proportional to the energy squared, in accordance with Eq. (4).

## III. FUNDAMENTAL ABSORPTION EDGE OF $Ga_{1-x}Mn_xAs$

Below we will focus on $Ga_{1-x}Mn_xAs$ grown by the low temperature (LT) molecular beam epitaxy technique.[20] For this material there are two sources of disorder. LT growth of GaAs is known to produce material with a high concentration of As antisites, yielding a high degree of disorder. On the other hand Mn ions incorporated into GaAs on the level of a few molar percent contribute additionally to the crystal disorder.

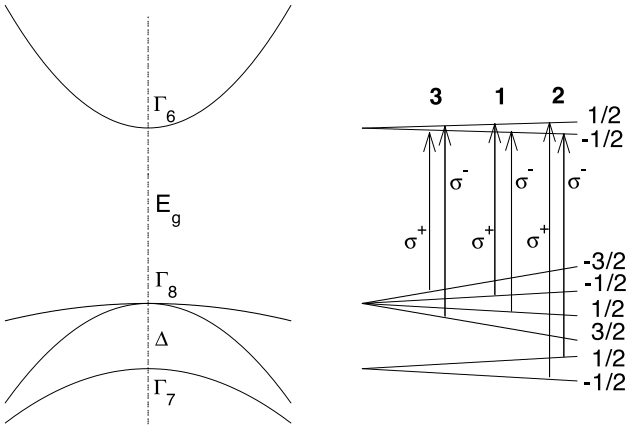


FIG. 2. Energy band structure of zinc-blende-type diluted magnetic semiconductor in the vicinity of the Brillouin zone Γ point. The right panel shows the allowed interband optical transitions in the Faraday configuration under external magnetic field. $\sigma^+$ and $\sigma^-$ transitions are marked. The bold numbers give the relative intensities.

One of the most attractive features of $Ga_{1-x}Mn_xAs$ is its DMS-type behavior, i.e., strong interaction between delocalized *s*- and *p*-type band electrons and localized *d*-type electrons of the magnetic ions (so called *s*, *p*-*d* exchange interaction). In particular, this interaction yields band splittings of the order of 100 meV, which corresponds to an effective *g* factor of a few hundreds.[10,15] The interaction for the conduction band (*s*-*d* exchange) is driven by direct potential exchange and should always be ferromagnetic (FM),[21] which is indeed the case for all DMS examples known so far.[10,22] On the other hand, valence band *p*-*d* exchange is dominated by the kinetic exchange mechanism and can be both ferromagnetic and antiferromagnetic (AFM), depending on exchange channels, i.e., available paths for virtual electron jumps between the valence band and *d* orbitals.[22,23]

The energy band structure of a zinc-blende-type diluted magnetic semiconductor in the vicinity of the Γ point is shown in Fig. 2. The exchange interaction induces bands splitting. The energies of the electronic transitions to the conduction band from the heavy holes $E_{hh\text{-}c}$, light holes $E_{lh\text{-}c}$, and spin-orbit split band $E_{so\text{-}c}$ in $\sigma^+$ and $\sigma^-$ polarized light in the vicinity of the Γ point are as follows.[24] For $\sigma^+$,

$$E_{hh\text{-}c,\sigma^+}=E_g+3b-3a,$$

$$E_{lh\text{-}c,\sigma^+}=E_g+b+3a,$$

$$E_{so\text{-}c,\sigma^+}=E_g-b+3a,$$

and for $\sigma^-$,

$$E_{hh\text{-}c,\sigma^-}=E_g-3b+3a,$$

$$E_{lh\text{-}c,\sigma^-}=E_g-b-3a,$$

$$E_{so\text{-}c,\sigma^-}=E_g+b-3a, \qquad (10a)$$

where

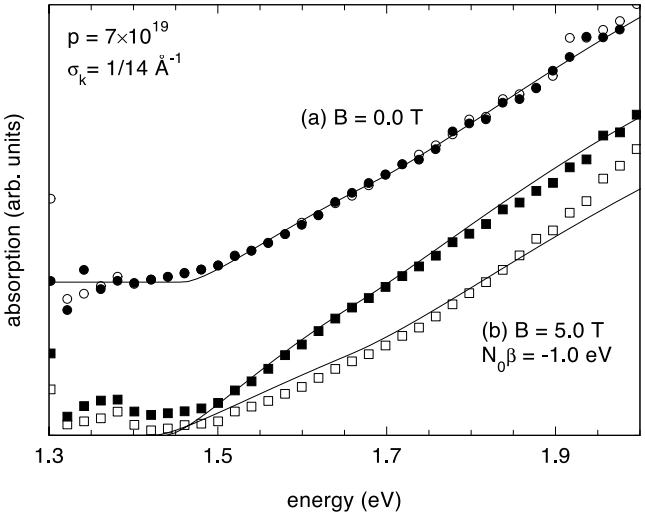


FIG. 3. The absorption coefficient of $Ga_{1-x}Mn_xAs$ ($x=0.032$). The experimental data are shown by points (Ref. 12). The open (closed) symbols correspond to $\sigma^+$ ($\sigma^-$) polarization of light. The zero field absorption data (a) are moved up relative to the measurements at 5.0 T (b) for clarity. The results of the model calculations for each polarization are presented by solid lines. The values of $p=7.0\times10^{19}$ cm$^{-3}$, $N_0\beta=0.0$ (a), $N_0\beta=-1.0$ eV (b), and $\sigma_k=1/14$ Å$^{-1}$ were used.

$$a=\tfrac{1}{6}N_0\alpha x\langle -S\rangle, \quad b=\tfrac{1}{6}N_0\beta x\ \langle -S\rangle. \qquad (10b)$$

$N_0\alpha$ and $N_0\beta$ are the exchange integrals for the conduction (*s*-*d*) and valence bands (*p*-*d*), and $\langle S\rangle$ is the thermodynamic average of the spin *S* and is proportional to the magnetization of the system of magnetic ions.[10]

For $Ga_{1-x}Mn_xAs$ epilayers ($x\approx0.03$–$0.04$) the *p*-*d* exchange interaction was found to be antiferromagnetic ($N_0\beta<0$).[15] Transmission was measured in the spectral range 1.4–2.0 eV, at temperatures 2 K$<T<$60 K, and magnetic field up to 5 T. Circularly polarized light ($\sigma^-$ and $\sigma^+$) was used. Detailed information about this experiment and the sample preparation can be found in Ref. 15.

The sample absorption spectra are shown (by points) in Fig. 3. Instead of a sharp absorption edge a broad, ramplike edge is observed. The highest value of the detectable absorption coefficient in this experiment was about $10^4$ cm$^{-1}$. Under external magnetic field the absorption edge splits by about 100 meV. Such strong edge splitting is characteristic for *s*, *p*-*d* exchange effects.[10,24] The $\sigma^-$ edge is redshifted with respect to the $\sigma^+$ edge, which is attributed to the Moss-Burstein shift.[15]

For epilayers with hole concentration ranging between $10^{18}$ and $10^{20}$ cm$^{-3}$, the fact that the top of the valence band is empty (filled with holes) must be taken into account, since the Fermi energy level *F* can be up to about 300 meV below the top of the valence band. Consequently the Moss-Burstein shift of the absorption edge becomes sizable and is different for transitions originating from different valence subbands split by *s*, *p*-*d* exchange interaction (Fig. 4). It appears that in this case, assuming direct transitions, for FM *s*-*d* exchange ($N_0\alpha>0$) and AFM *p*-*d* exchange ($N_0\beta<0$), $\sigma^+$

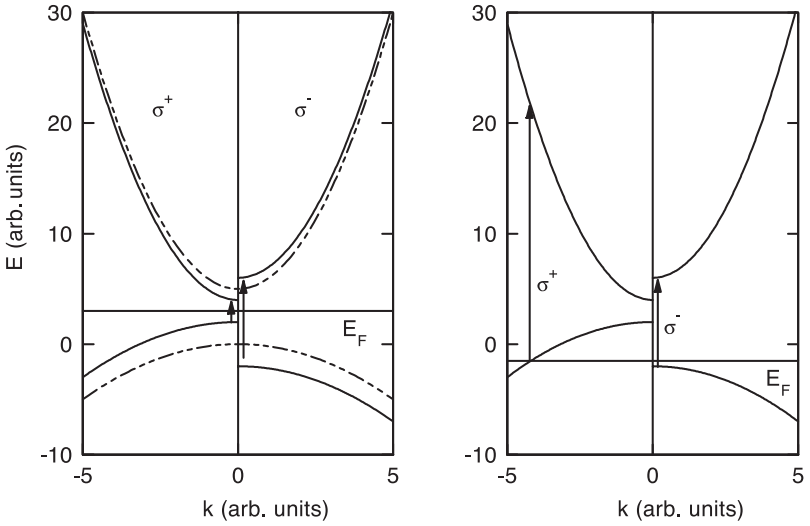


FIG. 4. Scheme of the $Ga_{1-x}Mn_xAs$ band structure (only conduction and heavy hole valence bands are shown) split by FM $s$-$d$ exchange ($N_0\alpha>0$) and AFM $p$-$d$ exchange ($N_0\beta<0$). The bands in the absence of the exchange interaction are denoted by dashed lines. Optical transitions for $\sigma^+$ and $\sigma^-$ transitions are shown in the case of low hole concentration (Fermi level in the energy gap, left panel) and for high hole concentration (Fermi level below top of the valence band, right panel).

transitions occur at higher energy than $\sigma^-$ ones, which is opposite to the situation for canonical DMS's (such as $Cd_{1-y}Mn_yTe$).[10,24] The Moss-Burstein shift is the primary reason for this splitting inversion. The role of $p$-$d$ interaction is to polarize the hole subbands, which differentiate the Moss-Burstein transition energies. We note that this model was recently repeated for GaMnAs in Ref. 33 assuming only direct transitions. The obtained squareroot-type absorption edge significantly differs from the measured absorption edge, as could have been expected.[15]

On the other hand magnetic circular dichroism reflectance and absorption experiments performed on $Ga_{1-x}Mn_xAs$ epilayers[13] and superlattices[25,14] show rather complicated spectra. In particular, the MCD for some samples can change its sign from negative to positive. This means that the $\sigma^+$ and $\sigma-$ absorption edges cross each other. We should note that MCD is very sample dependent. We will return to this point later.

## IV. RESULTS OF CALCULATIONS FOR FUNDAMENTAL ABSORPTION EDGE IN $Ga_{1-x}Mn_xAs$

Absorption was calculated according to Eq. (9) in the energy range up to 2.5 eV, for transitions from heavy holes, light holes, and spin-orbit split valence bands. We used pure GaAs band parameters and assumed parabolic bands for simplicity ($m_e=0.0665m_0$, $m_{hh}=0.47m_0$, $m_{lh}=0.082m_0$, $m_{so}=0.15m_0$). Renormalization of the energy gap caused by the high carrier concentration was adjusted to provide the best fit with the zero field experimental data. We neglected the band tailing, i.e., localized states in the energy gap. We also neglected any excitonic effects, because no excitons have been observed in $Ga_{1-x}Mn_xAs$ epilayers.

In the calculations we assumed the saturated magnetization limit, i.e., $\langle S\rangle=5/2$, which is reasonable for the sample considered for $B>1$ T. The $s$-$d$ exchange integral was chosen as typical for other DMS materials, $N_0\alpha=+0.2$ eV. The $p$-$d$ exchange integral $N_0\beta$ was considered as a fitting parameter. In order to reduce the number of parameters, we assumed $N_0\beta$ to be $\boldsymbol{k}$ vector independent, although it is known that for large $\boldsymbol{k}$ values $N_0\beta$ may be substantially reduced.[24] According to information from the crystal growth process the manganese concentration in the sample was $x=0.032$. Since the concentrations of free holes in the samples were not known precisely,[20,26] we allowed them to vary between $10^{19}$ and $10^{20}$ $cm^{-3}$, as suggested by the ferromagnetism of the samples.

The band splitting due to the exchange interaction was taken into account by calculating the Fermi energy in each subband (see Fig. 4). According to this model the upper limit for the integration in Eq. (9c) should be modified as follows:

$$k_c^{max}=\sqrt{\frac{2m_v}{\hbar^2}(\hbar\omega-F'-E_g')}, \tag{11}$$

where $F'$ is the Fermi energy relative to the top of the considered valence subband and $E_g'$ is equal to the effective band gap calculated according to Eq. (10) and modified by the many-body effect band gap renormalization (assumed to be equal for all subbands). The standard absorption intensity ratio between heavy holes, light holes, and spin-orbit bands (3:1:2) was used.

In Fig. 5 we present some results of calculations of the fundamental absorption edge for two sample hole concentrations and three different distribution width parameters $\sigma_k$. For very small values of the $\sigma_k=\sigma_1$ parameter the heavy holes, light holes, and spin-orbit band transitions are clearly distinguishable. In this case the crystal starts to absorb light at the energy $E_0=E_g+\hbar^2k_F^2/2m_c+\hbar^2k_F^2/2m_v$, where $k_F$ is the wave vector corresponding to the Fermi energy in the valence band. Thus for a $p$-type semiconductor $E_0$ is governed mostly by the effective mass of the conduction band, because $\hbar^2k_F^2/2m_c\gg\hbar^2k_F^2/2m_v$ when $m_c\ll m_v$ (compare Fig. 4).

However, for larger $\sigma_k=\sigma_2,\sigma_3$ the absorption edge becomes smoother, and the sample absorbs light of energy $E_0\approx E_g+\hbar^2k_F^2/2m_v$, since indirect transitions are also allowed and the absorption edge corresponds to the energy difference between occupied and empty states.

To compare our calculations with the experimental data we used four independent parameters. These are the free hole concentration $p$, the energy gap (including gap renormalization) $E_g$ of $Ga_{1-x}Mn_xAs$, the value of the $p$-$d$ exchange integral $N_0\beta$, and the parameter of the quasimomentum dis-

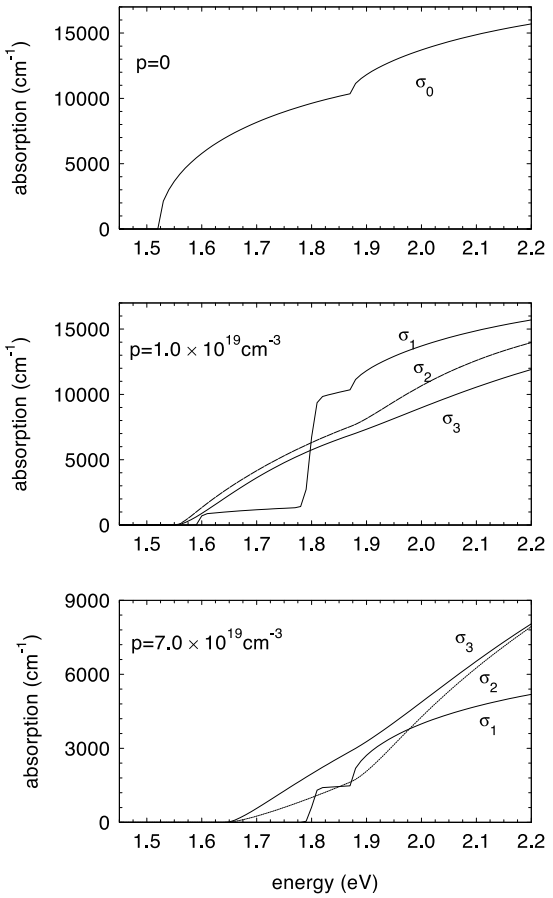


FIG. 5. The calculated fundamental absorption edge in the case of large free hole concentration ($p=1.0\times10^{19}$ cm$^{-3}$ and $p=7.0\times10^{19}$ cm$^{-3}$). The Moss-Burstein effect is taken into account according to Eq. (11). Isotropic and parabolic bands are assumed. Excitonic effects are neglected. For very small values of the $\sigma_k$ parameter the heavy holes, light holes, and spin-orbit band transitions are clearly visible. We used three $\sigma_k$ parameters: $\sigma_1$ corresponding to the Bohr radius of the donor ($a_D^*=104$ Å), $\sigma_2$ for an object with size $a^*=25$ Å, and $\sigma_3$ for the acceptor ($a_A^*=14.8$ Å). As a reference the curve for the undoped semiconductor ($p=0$) is also shown ($\sigma_0=0.001$ Å$^{-1}$).

persion $\sigma_k$. In the magnetotransmission experiment considered the relative absorption coefficient was measured (arbitrary units were used[15]), so we normalized our spectra and the coefficient $A$ in the matrix element [Eq. (7)].

In Fig. 3 we present the results of the calculations together with the experimental data in the absence (a) as well as in the presence (b) of an external magnetic field. For $B=0$ a reasonable matching was obtained for the following parameters: free hole concentration $p=7.0\times10^{19}$ cm$^{-3}$ (well within the expected range) and $\sigma_k\simeq1/14$ Å$^{-1}$, very close to the value of the inverse Bohr radius of the acceptor in GaAs. Since the exact dependence of the energy gap on the Mn concentration in the mixed $Ga_{1-x}Mn_xAs$ crystal is not known, the renormalized energy gap[27] has to be adjusted as well. We obtained $E_g=1.31$ eV, in reasonable agreement with the tendency for many-body energy gap shrinkage expected for such a carrier concentration (for $p=7.0\times10^{19}$ cm$^{-3}$ $E_g=1.41$ eV, calculated for GaAs from Ref. 27). Using the parameters obtained for $B=0$ we fitted the absorption edge split by a magnetic field and obtained $N_0\beta=-1.0$ eV.

There are two points that we would like to stress. The first is that the calculations predict a ramplike absorption edge, as observed in experiment. The second is the reasonable description of the exchange induced splitting with the parameters $N_0\alpha=+0.2$ eV and $N_0\beta=-1.0$ eV. The sign of the latter is particularly important, since it proves antiferromagnetic $p$-$d$ exchange in $Ga_{1-x}Mn_xAs$ epilayers as expected for $Mn^{2+}$ ($d^5$) centers. Moreover, the magnitude of this interaction is rather typical of other DMS's.[10,21,24]

We would like to mention the transmission experiments at the fundamental absorption edge performed on low temperature GaAs.[28] The absorption edge of this material was also found to be very broad, as for $Ga_{1-x}Mn_xAs$ (zero field data) presented in Fig. 3(a). This may suggest that the primary reason for the disorder in LT GaAs and LT $Ga_{1-x}Mn_xAs$ is the same. In such a case the likely candidate would be the As antisite. In other words, low temperature technology produces so many defects ($As_{Ga}$) that addition of Mn increases the disorder only slightly.

## V. RESULTS OF CALCULATIONS OF MAGNETIC CIRCULAR DICHROISM

It is known for $Ga_{1-x}Mn_xAs$ that depending on the growth conditions one can grow samples with the same manganese concentration, but with different magnetic and electrical properties,[20] from metalliclike ferromagnetic to semiinsulating paramagnetic samples. Therefore it is likely that apart from the manganese acceptor centers in $Ga_{1-x}Mn_xAs$ there are also many other centers of yet unknown origin. However, the presence of those centers may strongly influence the shape of the fundamental absorption edge. Since the disorder inside the crystal lattice depends on the number and nature of the centers, $\sigma_k$ can also be very different in different samples. This conclusion also concerns the hole concentration $p$ of the sample. The variety of MCD spectra reported so far seem to corroborate this expectation.

Magnetic circular dichroism experiments measure the difference between the intensity of the light in the polarizations $\sigma^-$ and $\sigma^+$. Measurements performed on thin $Ga_{1-x}Mn_xAs$ samples show that in the fundamental absorption edge range the MCD signal can have negative or positive sign, which means that the $\sigma^-$ and $\sigma^+$ absorption edges in some cases cross each other.[14,29–32]

In Fig. 6 we present the results of model calculations of $Ga_{1-x}Mn_xAs$ MCD spectra [MCD calculated as $(I_{\sigma^+}-I_{\sigma^-})/(I_{\sigma^+}+I_{\sigma^-})$, where $I_{\sigma^-}$ and $I_{\sigma^+}$ are the light intensities in $\sigma^-$ and $\sigma^+$ polarization]. We used the same set of parameters as for the absorption edge calculations.

In the case of transitions from the top of the valence band (the absence of free holes $p=0$) the MCD signal is negative for any $\sigma_k$ value, as expected (Fig. 6, $p=0$).

For low hole concentration ($p=5.0\times10^{18}$ cm$^{-3}$ and $p=1.0\times10^{19}$ cm$^{-3}$) and small $\sigma_k=\sigma_1$ (direct absorption limit) the Moss-Burstain effect is small. The $p$-$d$ exchange

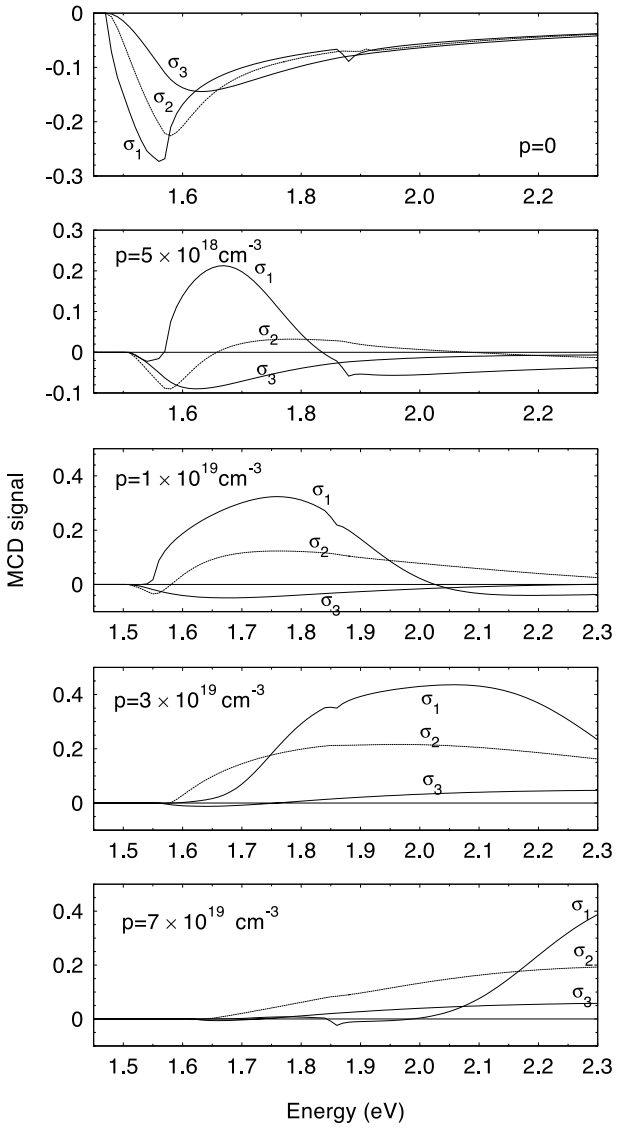


FIG. 6. Transmission MCD spectra calculated as $(I_{\sigma^-}-I_{\sigma^+})/(I_{\sigma^-}+I_{\sigma^+})$ for $\sigma^-$ and $\sigma^+$ light polarization for $Ga_{1-x}Mn_xAs$ ($x=0.032$) for different values of free hole concentration $p=0$ cm$^{-3}$, $p=5.0\times10^{18}$cm$^{-3}$, $p=1.0\times10^{19}$ cm$^{-3}$, $p=3.0\times10^{19}$ cm$^{-3}$, $p=7.0\times10^{19}$cm$^{-3}$. For each concentration three values of the $\sigma_k$ parameter were taken: $\sigma_k=(100\ \text{Å})^{-1}$ (bold line), $\sigma_k=(25\ \text{Å})^{-1}$ (dotted line), $\sigma_k=(10\ \text{Å})^{-1}$ (thin line). Exchange integrals $N_0\alpha=0.2$ eV and $N_0\beta=-1.0$ eV are assumed. The structure around 1.85–1.90 eV comes from the transitions from the spin-orbit split band.

interaction is strong enough to completely polarize the holes, i.e., the Fermi energy $F$ is between the heavy hole subbands. The $\sigma^-$ transition occurs at the top of the valence band, as depicted in Fig. 4, right panel. Therefore the transition observed in $\sigma^+$ polarization is at higher energy than the $\sigma^-$ transition, and the sign of the MCD becomes positive (cf. Fig. 4). However, for larger $\sigma_k$(***k***-selection rule is released) indirect transitions are also allowed and the most important is the energy difference between occupied and empty states. This leads to a reversal of the MCD sign, which becomes negative.

The evolution of MCD with still higher hole concentration is shown in Fig. 6 for $p=3\times10^{19}$ and $p=7\times10^{19}$ cm$^{-3}$. In the case of the highest hole concentration ($p=7.0\times10^{19}$ cm$^{-3}$) the Fermi energy is below the top of both valence subbands shown in Fig. 4 and the exchange interaction cannot polarize the holes completely. Therefore for higher photon energies, as long as we consider only transitions from $\Gamma_8$ and $\Gamma_7$ to $\Gamma_6$, the MCD signal is always positive (for negative $N_0\beta$), which is the case for all known $Ga_{1-x}Mn_xAs$ samples. However, for low photon energies, slightly above $E_g$, and for relatively large values of $\sigma_k$ (the released ***k***-selection rule), once more we get a reversal of the sign of the MCD. In such a situation the energy difference between occupied and empty states is lower for transitions in $\sigma^+$ polarization than for $\sigma^-$, and this is the reason why the MCD signal is slightly negative (Fig. 6, $p=7\times10^{19}$).

From our simulations it is apparent that the results of MCD experiments are very sensitive to the sample properties, such as hole concentration and disorder parametrized by $\sigma_k$. For instance, for samples with low hole concentration ($p=1.0\times10^{19}$ cm$^{-3}$) and intermediate value of the $\sigma_k$ parameter ($\sigma_k=25$ Å$^{-1}$) the MCD signal above the energy gap is negative, whereas for samples with higher concentrations of free holes ($p=3.0\times10^{19}$ and $p=7.0\times10^{19}$ cm$^{-3}$), the signal appears to be positive. Thus it is difficult to draw conclusions about the sign of the exchange integral $N_0\beta$ from only the sign of the MCD signal, without taking into account any information about the concentration of the carriers and the ''magnitude'' of the disorder.

## VI. CONCLUSIONS

A model for the calculation of the fundamental absorption edge in heavily doped semiconductors is proposed. The aim of the model is to replace the quasimomentum conservation by a certain ***k***-vector distribution. Using the presented model for optical absorption in random media one can reproduce the results of transmission measurements on heavily doped or disordered semiconductors, as was shown for $Ga_{1-x}Mn_xAs$ epilayers. Without a microscopic model of disorder we are not in a position to determine parameters such as the width of the $k$ vector distribution $\sigma_k$. Theoretical work in this direction is currently in progress.

Since some parameters for $Ga_{1-x}Mn_xAs$—such as the carrier concentration or the value of the energy gap—are not known with reasonable accuracy, the $p$-$d$ exchange integral for this material cannot be evaluated precisely. However, the results of the present calculation of the fundamental absorption edge for $Ga_{1-x}Mn_xAs$ epilayers strongly suggest an antiferromagnetic $p$-$d$ exchange interaction ($N_0\beta<0$).

## ACKNOWLEDGMENTS

We acknowledge partial support by the Polish Committee for Scientific Research (KBN), in particular under Grant No. 2 P03B 110 16. One of us (J.S.) acknowledges support from the Foundation for Polish Science (FNP).

[1] G. Lasher and F. Stern, Phys. Rev. **133**, A553 (1964).
[2] D. M. Eagles, Phys. Chem. Solids **16**, 76 (1960).
[3] G. Gobel, Appl. Phys. Lett. **24**, 492 (1974).
[4] L. Bonch-Bruevich, Fiz. Tverd. Tela. (Leningrad) **4**, 2660 (1962) [Sov. Phys. Solid State **4**, 1953 (1963)].
[5] E. O. Kane, Phys. Rev. **131**, 79 (1963).
[6] I. M. Lifshitz, Zh. Éksp. Teor. Fiz. **44**, 1723 (1963) [Sov. Phys. JETP **17**, 1159 (1963)].
[7] B. I. Halperin and M. Lax, Phys. Rev. **148**, 722 (1966).
[8] A. A. Klochikhin, Phys. Rev. B **52**, 10 979 (1995).
[9] J. Singh, Phys. Rev. B **23**, 4156 (1981).
[10] *Semiconductors and Semimetals*, Vol. 25 of *Diluted Magnetic Semiconductors*, edited by J. K. Furdyna and J. Kossut (Academic Press, New York, 1988); *Diluted Magnetic Semiconductors*, edited by M. Balkanski and M. Averous (Plenum Press, New York, 1991); J. Kossut and W. Dobrowolski, in *Handbook of Magnetic Materials*, edited by K. H. J. Buschow (North-Holland, Amsterdam, 1993), Vol. 7, p. 231; J. Kossut and W. Dobrowolski, in *Narrow Gap II-VI Compounds for Optoelectronic and Electromagnetic Applications*, edited by P. Capper (Chapman & Hall, London, 1997).
[11] H. Ohno, Science **281**, 951 (1998), and references therein.
[12] H. Ohno, J. Magn. Magn. Mater. **200**, 110 (1999).
[13] K. Ando, T. Hayashi, M. Tanaka, and A. Twardowski, J. Appl. Phys. **83**, 6548 (1998).
[14] B. Beschoten, P. A. Crowell, I. Malajovich, D. D. Awschalom, F. Matsukura, A. Shen, and H. Ohno, Phys. Rev. Lett. **83**, 3073 (1999).
[15] J. Szczytko, W. Mac, A. Twardowski, F. Matsukura, and H. Ohno, Phys. Rev. B **59**, 12 935 (1999).
[16] O. Madelung, *Introduction to Solid State Theory* (Springer, Berlin, 1996).
[17] E. O. Kane, Phys. Chem. Solids **1**, 249 (1957).
[18] M. Osinski and M. J. Adams, IEE Proc., Part I: Solid-State Electron Devices **129**, 229 (1982).
[19] W. P. Dumke, Phys. Rev. **132**, 1998 (1963).
[20] H. Munekata, H. Ohno, S. von Molnar, A. Segmuller, L. L. Chang, and L. Esaki, Phys. Rev. Lett. **63**, 1849 (1989); H. Munekata, H. Ohno, S. von Molnar, A. Harwit, A. Segmuller, and L. L. Chang, J. Vac. Sci. Technol. B **8**, 176 (1990); S. Koshihara, A. Oiwa, M. Hirasawa, S. Katsumoto, Y. Iye, C. Urano, H. Takagi, and H. Munekata, Phys. Rev. Lett. **78**, 4617 (1997).
[21] K. Hass, in *Diluted Magnetic Semiconductors* (Ref. 10).
[22] A. Twardowski, D. Heiman, M. T. Liu, Y. Shapira, and M. Demianiuk, Phys. Rev. B **53**, 10 728 (1996).
[23] J. Blinowski and P. Kacman, Phys. Rev. B **46**, 12 298 (1992); A. K. Bhattacharjee, *ibid.* **46**, 5266 (1992); **49**, 13 978 (1994).
[24] J. P. Lascaray, in *Diluted Magnetic Semiconductors* (Ref. 10).
[25] T. Hayashi, M. Tanaka, K. Seto, T. Nishinaga, and K. Ando, Appl. Phys. Lett. **71**, 1825 (1997).
[26] T. Omiya, F. Matsukura, T. Dietl, Y. Ohno, T. Sakon, M. Motokawa, and H. Ohno, Physica E Amsterdam **7**, 976 (2000).
[27] B. R. Bennet, R. A. Soref, and J. A. del Alamo, IEEE J. Quantum Electron. **26**, 113 (1990).
[28] S. U. Dankowski, D. Streb, M. Ruff, P. Kiesel, M. Kneissl, B. Knupfer, G. H. Duhler, U. D. Keil, C. B. Sørensen, and A. K. Verma, Appl. Phys. Lett. **68**, 37 (1996); S. U. Dankowski, P. Kiesel, M. Ruff, D. Streb, S. Tautz, U. D. Keil, C. B. Sørensen, B. Knupfer, M. Kneissl, and G. H. Duhler, Mater. Sci. Eng., B **44**, 316 (1997).
[29] M. Tanaka, H. Shimizu, T. Hayashi, H. Shimada, and K. Ando, J. Vac. Sci. Technol. A **18**, 1247 (2000).
[30] M. Tanaka, J. Vac. Sci. Technol. B **16**, 2267 (1998).
[31] T. Hayashi, M. Tanaka, K. Seto, T. Nishinaga, and K. Ando, Appl. Phys. Lett. **71**, 1825 (1997).
[32] H. Shimizu, T. Hayashi, T. Nishinaga, and M. Tanaka, J. Magn. Soc. Jpn. **23**, 96 (1999).
[33] T. Dietl, H. Ohno, and F. Matsukura, Phys. Rev. B **63**, 195205 (2001).